

Performance of a Discontinuous Galerkin Solver for Semiconductor Boltzmann Equations

Yingda Cheng

and Irene M. Gamba

Department of Mathematics and ICES

The University of Texas at Austin

Austin, TX 78712, USA

Email: ycheng@math.utexas.edu

Email: gamba@math.utexas.edu

Armando Majorana

Dipartimento di Matematica e Informatica

Università di Catania

Catania, Italy

Email: majorana@dmi.unict.it

Chi-Wang Shu

Division of Applied Mathematics

Brown University

Providence, RI 02912, USA

Email: shu@dam.brown.edu

Abstract—We present the effectiveness and competitiveness of a discontinuous Galerkin (DG) scheme applied to deterministic computations of the transients for the Boltzmann-Poisson (BP) system describing electron transport in semiconductor devices. In particular, we show that the scheme can maintain reasonable accuracy even with rather coarse meshes, hence providing a good alternative to the traditional DSMC solvers. Comparative studies for one-dimensional devices and simulations on a 2D double gate MOSFET are provided.

I. INTRODUCTION

In modern electron devices the scale length of individual components becomes comparable with the distance between successive carrier interactions with the crystal. A consistent statistical description of the dynamics of carriers is essential for a deeper understanding of the observed transport properties. For this purpose the semi-classical Boltzmann-Poisson system is used and given by

$$\frac{\partial f}{\partial t} + \frac{1}{\hbar} \nabla_{\mathbf{k}} \varepsilon \cdot \nabla_{\mathbf{x}} f - \frac{q}{\hbar} \mathbf{E} \cdot \nabla_{\mathbf{k}} f = Q(f), \quad (1)$$

$$\nabla_{\mathbf{x}} [\varepsilon_r(\mathbf{x}) \mathbf{E}] = -\frac{q}{\varepsilon_0} [\rho(t, \mathbf{x}) - N_D(\mathbf{x})], \quad (2)$$

which provides a general theoretical framework for modeling electron transport in electronic energy bands $\varepsilon = \varepsilon(\mathbf{k})$ associated to the crystal lattice. In Eq. (1), f represents the electron probability density function (*pdf*) in phase space \mathbf{k} at the physical location \mathbf{x} and time t . \mathbf{E} is the electric field, $Q(f)$ denotes the collision operator, which describes electron-phonon interactions and ε is the energy-band function. Physical constants \hbar and q are the Planck constant divided by 2π and the positive electric charge, respectively. In Eq. (2), ε_0 is the dielectric constant in the vacuum, $\varepsilon_r(\mathbf{x})$ labels the relative dielectric function depending on the material, $\rho(t, \mathbf{x})$ is the electron density, and $N_D(\mathbf{x})$ is the doping. The term $Q(f)$ models the collisional integral given by a classical linear operator with scattering mechanisms satisfying the Fermi's Golden rule accounting for acoustical (elastic) and absorption and emission (inelastic) transition rates (see [4] for a detailed description of the model).

The kinetic equation (1) is an equation in six dimensions (plus time if the model is not in steady state) for a truly

3-D device. Such high problem dimensionality and expected heavy computational cost have explained why the BP system is traditionally simulated by the Direct Simulation Monte Carlo (DSMC) methods [1].

After the pioneer work [6], in recent years, deterministic solvers to the BP system were proposed [2]–[5], [7]–[10]. These methods provide accurate results which, in general, agree well with those obtained from Monte Carlo (DSMC) simulations, often at a fractional computational time. Moreover, they can resolve transient details for the electron probability density function f , which are difficult to compute with DSMC simulators. The use of the discontinuous Galerkin (DG) method as we proposed in [4] for solving Eqs. (1)-(2) have considerable advantages over DSMC, including competitive computational cost for comparable resolution. We recall that the DG method is a finite element based approach that uses discontinuous piecewise polynomials as basis functions and relies on an adequate choice of numerical fluxes that handle effectively the interactions across element boundaries. They have been developed as an extraordinarily and highly adaptable computational tool which are stable and accurate for solving nonlinear hyperbolic conservation laws, nonlinear convection diffusion equations, etc.. We refer to [4] for a detailed description of our scheme for solving Eqs. (1)-(2) and examples of applications of this DG scheme to 1D diode and 2D double gate MOSFET devices. A review on DG methods for BP system can be found in a recent review paper [11]. In the present paper, we will demonstrate the effectiveness and competitiveness of our computational approach in term of maintaining accuracy for considerable coarse meshes and optimal computational times compared to DSMC solvers.

II. NUMERICAL RESULTS

Following [4] and previous related work referenced therein, we introduce a set of spherical coordinates using the wave vector $\mathbf{k} = \kappa \sqrt{r}(\mu, \sqrt{1 - \mu^2} \cos \varphi, \sqrt{1 - \mu^2} \sin \varphi)$, with $r \geq 0$, $\mu \in [-1, 1]$ and $\varphi \in [-\pi, \pi]$, where $\kappa = \hbar^{-1} \sqrt{2m^* k_B T_L}$, m^* is the effective electron mass, k_B is the Boltzmann constant and T_L the constant lattice temperature.

A. A one-dimensional device

First we will show the one-dimensional bulk device with an applied electric field of $10kV/cm$ to benchmark our scheme. We assume the Maxwellian distribution function at the initial time. The evolution of the mean velocity and mean energy is shown in Fig. 1 for a comparison between coarse and refined grids. The agreement is remarkably good given that the coarse mesh has only 8 cells in the μ -direction. The table below describes the relative error of the quantities for different grids with respect to the most refined grid 80×24 . Here, N_r , N_μ are the number of cells in r and μ directions, respectively. Fig. 2 shows the distribution function as a function of r and μ during the transient at time $0.4ps$. Notice that the variable φ is not considered for this problem due to the cylindrical symmetry.

N_r	N_μ	error in velocity	error in energy
80	16	$3.318e-03$	$2.541e-05$
80	12	$7.682e-03$	$4.423e-05$
80	8	$1.896e-02$	$5.557e-05$
40	24	$1.666e-03$	$8.509e-04$
40	16	$3.827e-03$	$8.334e-04$
40	12	$8.368e-03$	$8.344e-04$
40	8	$1.994e-02$	$8.848e-04$
20	24	$6.814e-03$	$2.749e-03$
20	16	$5.388e-03$	$2.766e-03$
20	12	$1.053e-02$	$2.797e-03$
20	8	$2.296e-02$	$2.907e-03$

B. A two-dimensional double gate MOSFET

Here we consider a double gate MOSFET device as shown in Figure 3. The top and bottom shadowed region denotes the oxide-silicon region, whereas the rest is the silicon region. We will only need to compute for $y > 0$ because of the symmetry of the problem. The electric potential $\Psi = 0$ at source, $\Psi = 1$ at drain and $\Psi = 0.5$ at gate. The relative dielectric constant in the oxide-silicon region is $\epsilon_r = 3.9$, in the silicon region is $\epsilon_r = 11.7$. The doping profile has been specified as follows: $N_D(x, y) = 1 \times 10^{17} cm^{-3}$ if $x < 50nm$ or $x > 100nm$, $N_D(x, y) = 5 \times 10^{14} cm^{-3}$ in the channel $50nm \leq x \leq 100nm$. All numerical results are obtained with piecewise linear polynomials and second order TVD Runge-Kutta time stepping. We use a very coarse mesh, 24×14 grid in space, 24 points in r , 8 points in μ and 6 points in φ in our calculation. In Figures 4 and 5, we show the macroscopic quantities for this device at equilibrium. In Figure 6, the transient state at $t = 0.05ps$ is given. We can identify some cells with negative energies. This numerical artifact is caused by a very coarse mesh we employed as well as the fact the gradient is really strong in this case. However, we want to remark that in [11], there are related discussions about the positivity of the solutions for BP systems. In general, if one uses only a piecewise constant approximation, then the solution will be positivity-preserving. However, for higher order approximations, this is no longer true and we observe it

here in the transient states. The way to remove this numerical artifact without sacrificing accuracy is discussed in [11], [12] and are subjects of future study for our application.

III. CONCLUSION

In this paper, we demonstrate the performance of DG schemes for BP systems under coarse meshes. We show that the results are quite satisfactory for the calculation of steady states, and the computational cost is small even for five-dimensional calculations. However, for some transient states, we expect to see some numerical artifacts caused by using a high order approximation on a very coarse mesh. This will be the subject of our future study.

ACKNOWLEDGMENTS

The first and second authors are partially supported by NSF DMS 1016001, 0757450 and 0807712. The third author thanks the support from the J. Tinsley Oden Faculty Research Fellowship and PRA 2009 Unict. The fourth author is supported by NSF DMS 0809086 and DOE DE-FG02-08ER25863. Support from the Institute for Computational Engineering and Sciences at the University of Texas at Austin is also gratefully acknowledged.

REFERENCES

- [1] C. Jacoboni and P. Lugli, *The Monte Carlo method for semiconductor device simulation*, Springer-Verlag: Wien-New York, 1989.
- [2] Y. Cheng, I. M. Gamba, A. Majorana, and C.-W. Shu, "Discontinuous Galerkin solver for the semiconductor Boltzmann equation," *SISPAD 07, June 14-17*, pp. 257–260, 2007.
- [3] —, "Discontinuous Galerkin solver for Boltzmann-Poisson transients," *J. Comput. Electron.*, vol. 7, pp. 119–123, 2008.
- [4] —, "A Discontinuous Galerkin solver for Boltzmann-Poisson systems for semiconductor devices," *Comput. Methods Appl. Mech. Eng.* vol. 198, pp. 3130–3150, 2009.
- [5] —, "A discontinuous Galerkin solver for full-band Boltzmann-Poisson models," *Proceeding of IWCE13*, pp. 211–214, 2009.
- [6] E. Fatemi and F. Odeh, "Upwind finite difference solution of Boltzmann equation applied to electron transport in semiconductor devices," *J. Comput. Phys.*, vol. 108, pp. 209–217, 1993.
- [7] J. A. Carrillo, I. M. Gamba, A. Majorana, and C.-W. Shu, "A WENO-solver for 1D non-stationary Boltzmann-Poisson system for semiconductor devices," *J. Comput. Electron.*, vol. 1, pp. 365–375, 2002.
- [8] —, "A WENO-solver for the transients of Boltzmann-Poisson system for semiconductor devices. performance and comparisons with Monte Carlo methods," *J. Comput. Phys.*, vol. 184, pp. 498–525, 2003.
- [9] —, "2D semiconductor device simulations by WENO-Boltzmann schemes: efficiency, boundary conditions and comparison to Monte Carlo methods," *J. Comput. Phys.*, vol. 214, pp. 55–80, 2006.
- [10] M. Galler and A. Majorana, "Deterministic and stochastic simulation of electron transport in semiconductors," *6th MAFPD (Kyoto) special issue Vol. 2*, pp. 349–365, 2007.
- [11] Y. Cheng, I. Gamba, A. Majorana and C.-W. Shu, *A brief survey of the discontinuous Galerkin method for the Boltzmann-Poisson equations*, preprint submitted to *Boletín de la Sociedad Española de Matemática Aplicada*, 2010.
- [12] Y. Cheng, I.M. Gamba and J. Proft, *Positivity-preserving discontinuous Galerkin schemes for linear Vlasov-Boltzmann transport equations*, preprint, 2010.

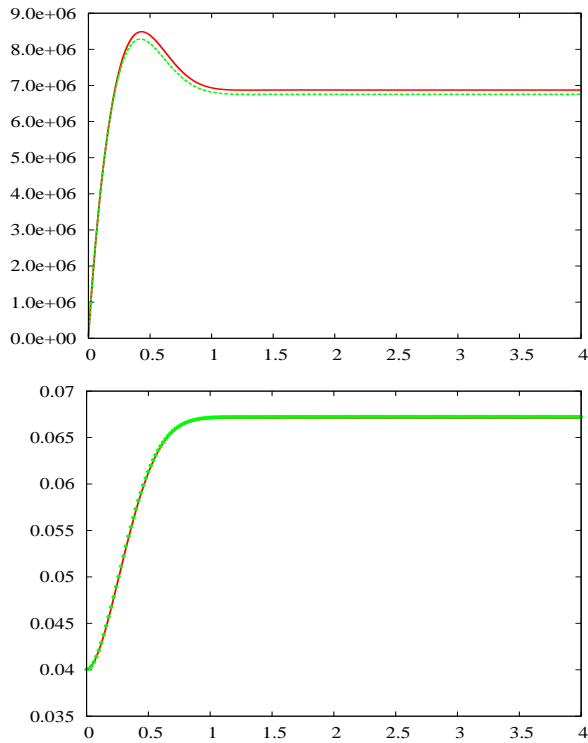


Fig. 1. Velocity in cm/s (top) and Mean energy in eV (bottom) on refined (80x24) and coarse (20x8) grid versus time in ps .

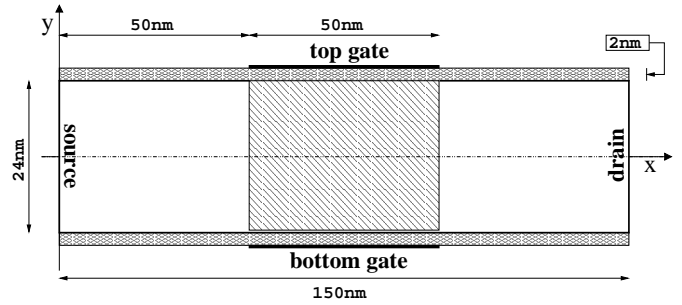


Fig. 3. Schematic representation of a 2D double gate MOSFET device

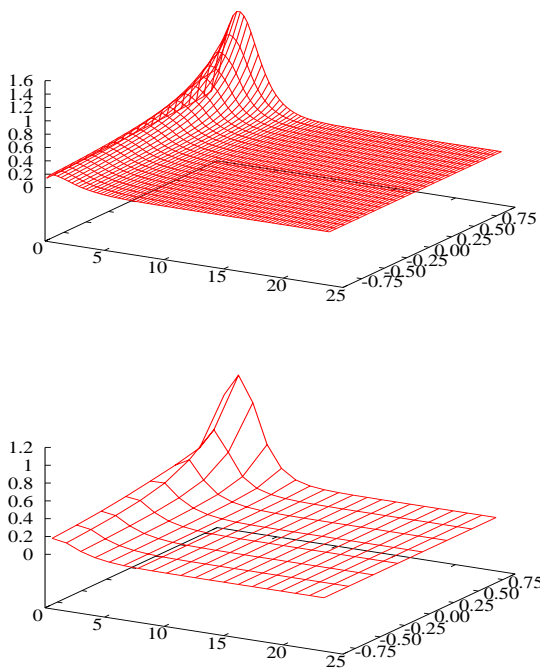


Fig. 2. Dimensionless distribution function. Top: refined grid: 80x24; bottom: coarse grid: 20x8.

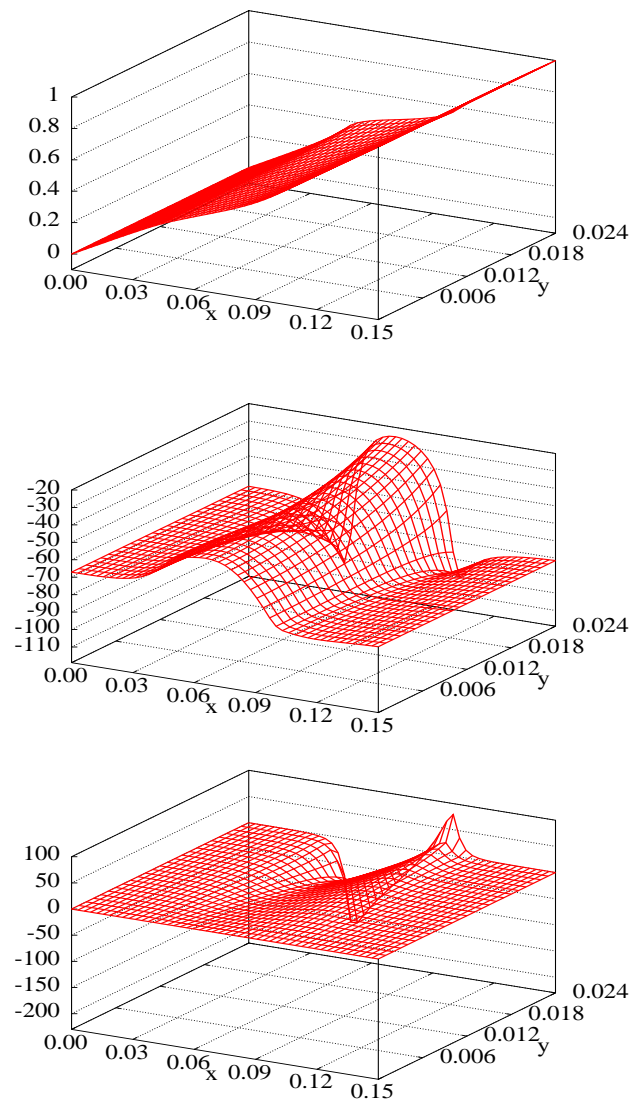


Fig. 4. 2D double gate MOSFET at equilibrium. $t = 2ps$. From top to bottom: potential in V , x-component of electric field in kV/cm , y-component of electric field in kV/cm .

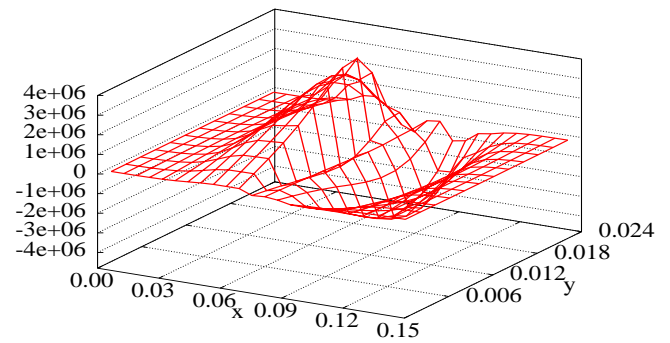
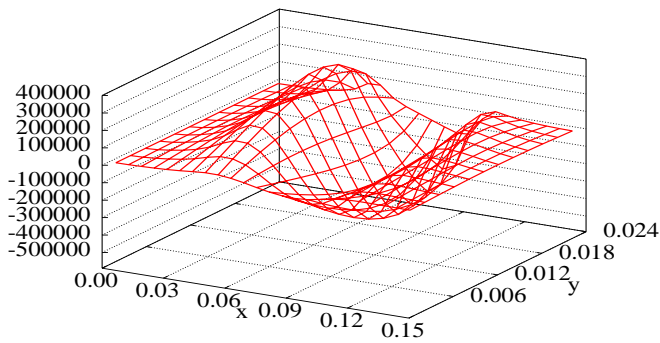
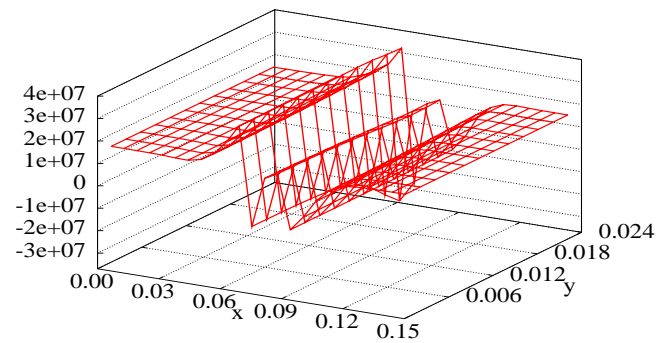
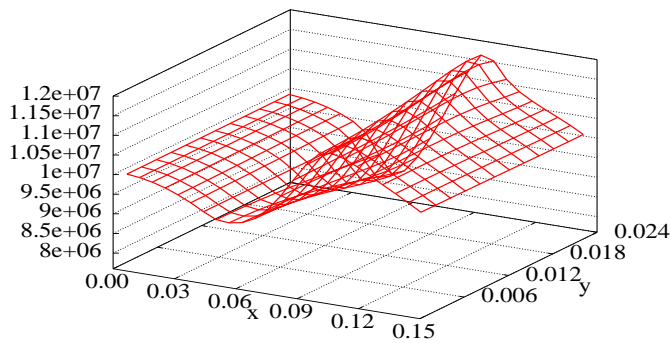
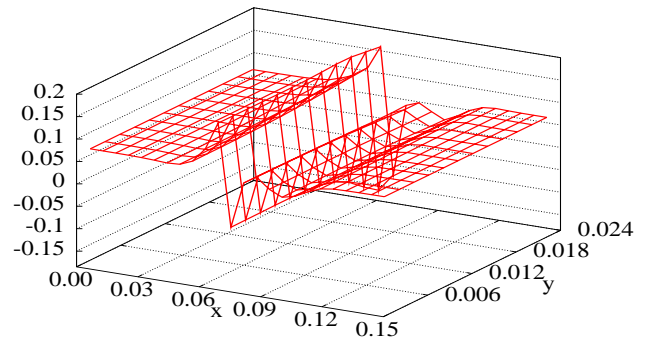
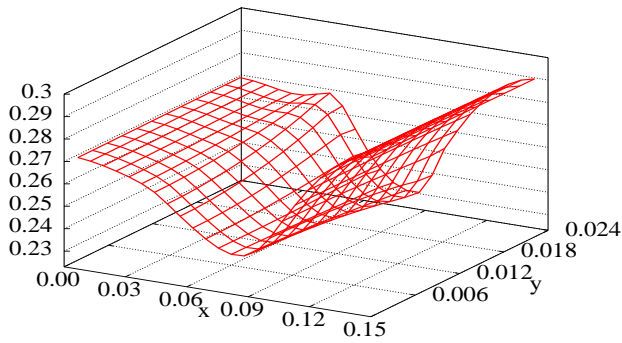
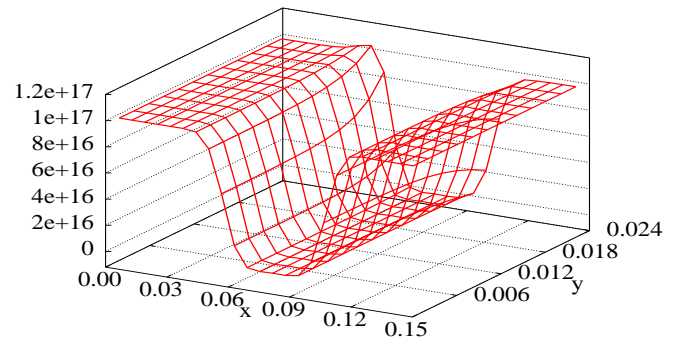
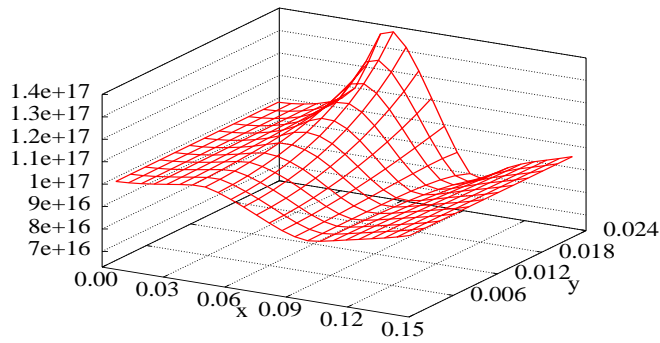


Fig. 5. 2D double gate MOSFET at equilibrium. $t = 2ps$. From top to bottom: density in cm^{-3} , energy in eV , x-component of velocity in cm/s , y-component of velocity in cm/s .

Fig. 6. 2D double gate MOSFET at $t = 0.05ps$. From top to bottom: density in cm^{-3} , energy in eV , x-component of velocity in cm/s , y-component of velocity in cm/s .